ChemComm

Accepted Manuscript

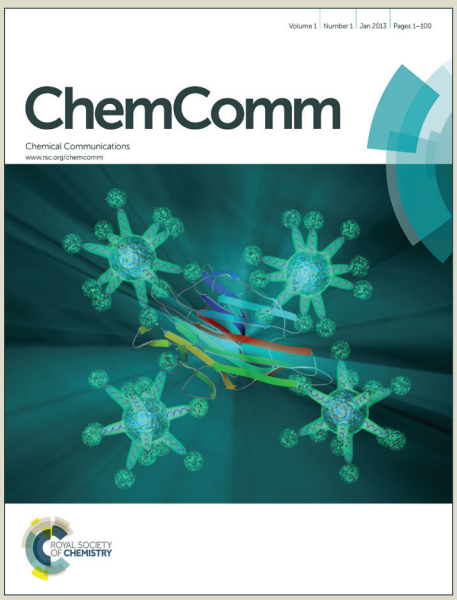

ROYAL SOCIETY OF CHEMISTRY

www.rsc.org/chemcomm

A fluorescent light-up probe with AIE characteristics for specific mitochondrial imaging to identify differentiating brown adipose cells

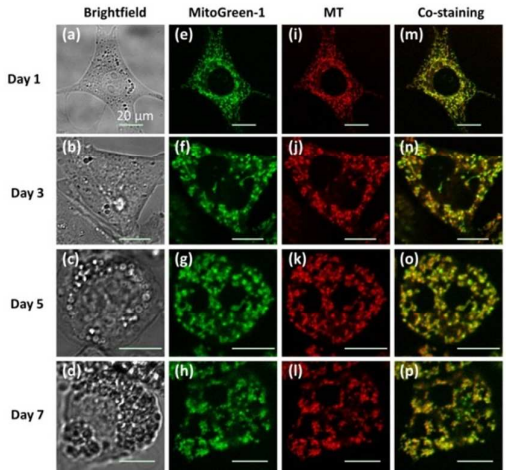

Cite this: DOI: 10.1039/c0xx00000x

www.rsc.org/xxxxxx

ARTICLE TYPE

A fluorescent light-up probe with AIE characteristics for specific mitochondrial imaging to identify differentiating brown adipose cells

Meng Gao,[‡a] Choon Kiat Sim,[‡b] Chris Wai Tung Leung,[c,d] Qinglian Hu,[e] Guangxue Feng,[e] Feng Xu,*[b,f] Ben Zhong Tang,*[c,d] and Bin Liu*[a,e]

Received (in XXX, XXX) Xth XXXXXXXXX 20XX, Accepted Xth XXXXXXXXX 20XX
DOI: 10.1039/b000000x

We report the design and synthesis of a specific mitochondrial fluorescent probe MitoGreen-1 with AIE characteristics to monitor the mitochondrial morphology changes and identify the differentiation process of living brown adipose cells. The probe AIE-MitoGreen-1 has significant advantages in high cell-permeability, good mitochondrial retention, low background fluorescence, large Stokes shift, and low toxicity.

There are two types of adipose cells in human: white adipose cells, which can store energy as triglycerides, and brown adipose cells, which can dissipate energy as heat.[1a] Recently, there is an increasing interest in understanding the differentiation process of brown adipose cells, which are critical for the treatment of obesity related diseases, such as type 2 diabetes, atherosclerosis, and cardiovascular disease.[1] Compared with positron emission tomography and magnetic resonance imaging methods,[2] fluorescence imaging gives unique advantages in high sensitivity, spatial and temporal detection abilities.[3] However, traditional fluorescence imaging methods for observing the differentiation process of brown adipose cells usually require lengthy processes: fixation, immunofluorescence with antibodies against specific proteins,[4] or transfection of DNA constructs encoding fluorescent proteins. [5] Therefore, it's highly desirable to develop a simple and minimally invasive imaging method for observing the differentiation process of brown adipose cells.

[a] *Institute of Materials Research Engineering (A*STAR), 3 Research Link, Singapore 117602;*
[b] *Singapore Institute for Clinical Sciences, Brenner Centre for Molecular Medicine (A*STAR), 30 Medical Drive, Singapore 117609*
[c] *Department of Chemistry, Division of Biomedical Engineering, The Hong Kong University of Science and Technology, Clear Water Bay, Kowloon, Hong Kong, China*
[d] *SCUT-HKUST Joint Research Laboratory, Guangdong Innovative Research Team, State Key Laboratory of Luminescent Materials & Devices, South China University of Technology, Guangzhou 510640, China*
[e] *Department of Chemical and Biomolecular Engineering, National University of Singapore, 4 Engineering Drive, Singapore 117576*
[f] *Department of Biochemistry, Yong Loo Lin School of Medicine, National University of Singapore, Singapore 117597*
† *Electronic Supplementary Information (ESI) available: General experimental procedures and characterization data for all compounds. See DOI: 10.1039/b000000x/*

‡*These authors contributed equally to this work.*

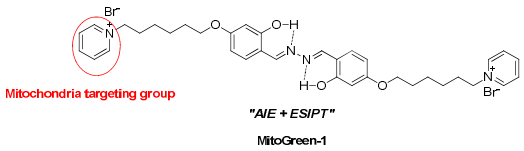

Scheme 1 Design of fluorescent mitochondrial probe **AIE-MitoGreen-1** with "AIE + ESIPT" characteristics.

A key characteristic of brown adipose cells during differentiation is that their mitochondrial content and activity will increase to accommodate the larger metabolic demands. By observing the changes in number, morphology and subcellular localizations of mitochondria through fluorescence imaging, it could provide a non-invasive method to identify the differentiation stages of brown adipose cells.[6] Although a variety of fluorescent dyes have been developed for mitochondrial imaging, such as rhodamines, rosamines, carbocyanines, styryl dyes, BODIPY and thiol-reactive Mitotracker dyes, they usually have large π–planar structures giving rise to small Stokes shifts (less than 40 nm), and their fluorescence would undergo self-quenching by high-concentration accumulation in mitochondria.[7] To tackle this challenge, a novel fluorescent probe **AIE-MitoGreen-1** has been designed on the basis of salicyladazine fluorophore[8] and positively charged pyridinium groups for specific mitochondrial imaging (Scheme 1).[9] The salicyladazine fluorophore uses two novel emission mechanisms: aggregation-induced emission (AIE) via restriction of intramolecular rotation around the *N*–*N* bond [10] and excited-state intramolecular proton transfer (ESIPT) via intramolecular hydrogen bonds.[11] As a result of these two mechanisms, they are non-emissive in dilute solutions but are highly emissive as nanoaggregates, which can be well retained in mitochondria without self-quenching effect and also produce a large Stokes shift (> 150 nm).

The synthetic procedure for **AIE-MitoGreen-1** is shown in Scheme 2. The reaction of 2,4-dihydroxybenzaldehyde **3** with 1,6-dibromohexane first generated compound **3** in 67% yield, which further reacted with hydrazine hydrate to afford the salicyladazine compound **4** in 85% yield. Compound **4**

further reacted with pyridine to afford the desired product **MitoGreen-1** in 93% yield. Their structures were confirmed with NMR and mass spectroscopies (see SI for details).

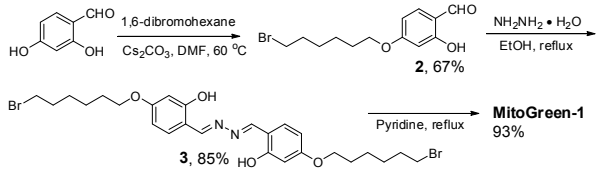

Scheme 2 Synthetic route for **MitoGreen-1**

Fig. 1 shows the photophysical properties of **AIE-MitoGreen-1**. An absorption maximum was seen at 356 nm in DMSO solution while an emission maximum was seen at 532 nm (Fig. 1A). This emission was strong at solid state, but it was almost zero in DMSO solution, suggesting that the emission is induced by aggregation. Moreover, the near-absence of overlap between the absorption and the emission spectra, shown by a large Stokes shift of 176 nm, suggests minimal self-absorption, a quality that is highly desirable for fluorescence imaging. The photoluminescence (PL) of **AIE-MitoGreen-1** was also tested in ethanol/hexane mixtures with different hexane fractions to fine-tune solvent polarity and solute aggregation (Fig. S1). As hexane was added to ethanol from 0 to 90 vol% to reduce polarity, the fluorescence signal of **AIE-MitoGreen-1** remains low (Fig. 1B). However, 99 *vol*% of hexane produced a 20-fold enhancement of emission, suggesting an AIE effect caused by the formation of **MitoGreen-1** aggregates with reduced solubility but not by the change of solvent polarity.

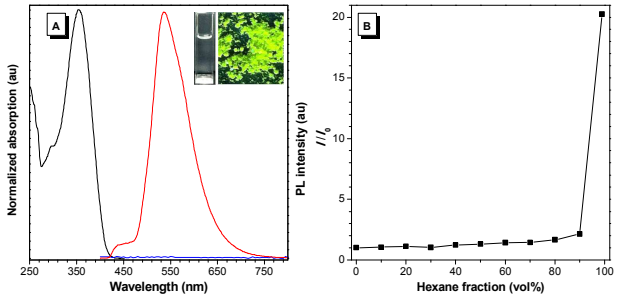

Fig. 1 (A) Normalized UV spectra of **AIE-MitoGreen-1** in DMSO solution (black); PL spectra of **AIE-MitoGreen-1** at solid state (red) and in DMSO solution (blue); (B) Plot of relative PL intensity (I/I_0, 532 nm) versus the solvent composition of ethanol/hexane mixture of **AIE-MitoGreen-1** .Concentration: 10 μM; excitation wavelength: 356 nm.

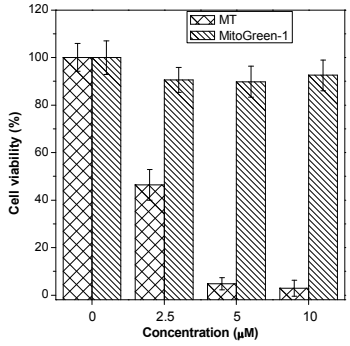

Fig. 2 Cytotoxicity experiments of **AIE-MitoGreen-1** and MT at various concentrations (0, 2.5, 5, 10 μM) in brown preadipose cells for 24 h.

The cytotoxicity of **AIE-MitoGreen-1** was evaluated by the widely used MTT assay. The samples were incubated with 0, 2.5, 5.0 and 10 μM **AIE-MitoGreen-1** for 24 hours, and the results showed that cell viabilities were close to 100% (Fig. 2). In contrast, only less than 10% of the cells were viable after incubation with 5.0 μM of a commercial mitochondrial dye, MitoTracker red FM (MT) for 24 hours, indicating that **AIE-MitoGreen-1** is much less cytotoxic than MT.

AIE-MitoGreen-1 was assessed for its ability to specifically localize in mitochondria of live brown preadipose cells by confocal fluorescence microscope. After incubation with 5 μM **AIE-MitoGreen-1** for 20 min (Fig. 3a), the tubular and reticular structures of mitochondria were clearly visible. The costaining experiment with MT showed an excellent overlap in the merged picture (Fig. 3b and 3c), suggesting that **AIE-MitoGreen-1** stains mitochondria specifically. The fact that compound **3** was not able to stain the brown preadipose cells suggested that the pyridinium groups were essential to achieve cellular intake and specific mitochondria imaging. To further explore whether **AIE-MitoGreen-1** can be used for direct *in situ* imaging of mitochondria, brown preadipose cells were incubated with **AIE-MitoGreen-1** for 20 min and imaged directly without washing. The fluorescence signals of **AIE-MitoGreen-1** were confined in mitochondria with negligible background signal from the culture medium (Fig. 3d), supporting the hypothesis that aggregated **AIE-MitoGreen-1** in the mitochondria gives higher fluorescence than the unaggregated forms in the medium. This specific staining of mitochondria remained even after incubation for 24 hour (Fig. 3e). In contrast, using the commercial MT probe without washing, a higher background signal was observed (Fig. 3f).These results clearly demonstrate that **AIE-MitoGreen-1** is suitable for specific and long-time tracing of mitochondria with high signal-to-background ratio and retention ability.

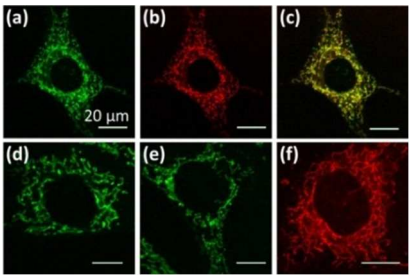

Fig. 3 Fluorescence images of brown preadipose cells stained with 5.0 μM **AIE-MitoGreen-1** and 50 nM MT: (a) Image from **AIE-MitoGreen-1**. (b) Image from MT. (c) Merged image of a and b. (d) Wash-free image from **AIE-MitoGreen-1** after 20 min. (e) Wash-free image from **AIE-MitoGreen-1** after 24 h. (f) Wash-free image of MT after 20 min. Scale bar = 20 μm. Excitation and emission wavelength: 405 nm and 500–550 nm for **AIE-MitoGreen-1;** 560 nm and 581–688 nm for MT.

Differentiation of brown preadipose cells was carried out with the previously described method.[12] The overall cellular morphology changed from a fibroblastic shape to a spherical shape (Fig. 4a–d). To visualize the mitochondria number and morphology changes during the differentiation process, 5 μM **AIE-MitoGreen-1** was added to the differentiation media at day 1, 3, 5, and 7. The changes of mitochondrial morphology and locations were shown by the confocal fluorescence images (Fig. 4e–h): at day 1 and 3, the mitochondria had a tubular and reticular morphology; at day 5 and 7 of differentiation, mitochondria appeared as punctate morphology. The specific imaging of **AIE-MitoGreen-1** for mitochondria during the differentiation process was also confirmed by the co-staining experiment with MT (Fig. 4i–p). Pearson's correlation coefficient (R_r; from +1 to −1), indicating the degree of linear dependence between two variables, is used to quantify the staining region overlap between **MitoGreen-1** and MT. Fluorescent signals of

the two dyes collected from two different channels are well overlapped with R_r = 0.80 (day 1), 0.85 (day 3), 0.86 (day 5), and 0.81 (day 7). The adipogenic differentiation of the cells was further confirmed by Oil-Red-O lipid staining, and the generation of lipid droplets could be clearly seen from day 3, a characteristic feature for successful adipogenic differentiation (Fig. S2).

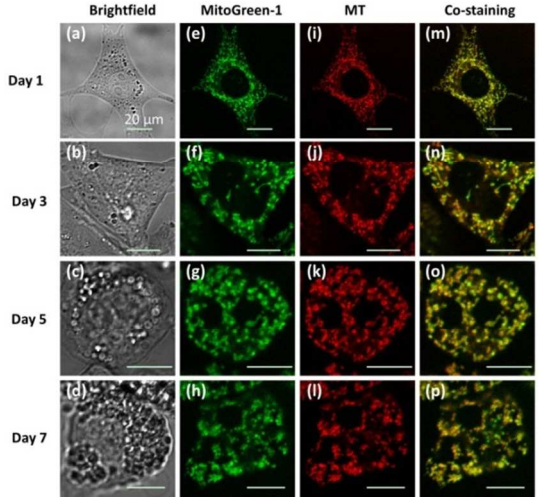

Fig. 4 Differentiating brown adipose cells (a–d, bright field) stained with **AIE-MitoGreen-1** (e–h, 5 μM) and MT (i–l, 50 nM), and their merged images (m–p). Scale bar = 20 μm. These images were obtained by confocal microscopy.

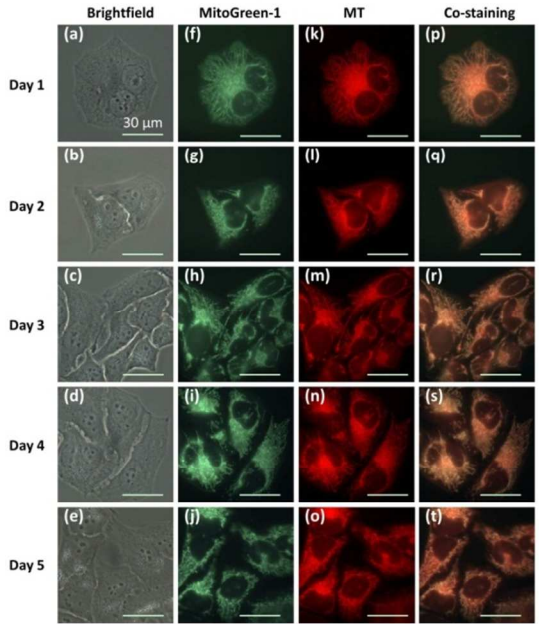

Fig. 5 HeLa cells (a–e, bright field) stained with **AIE-MitoGreen-1** (f–j, 5 μM) and MT (k–o, 50 nM), and their merged images (p–t). Scale bar = 30 μm. These images were obtained by fluorescence microscope.

To further demonstrate that the mitochondrial network changes are caused by the differentiation process, undifferentiating Hela cells were used as a control to show that their mitochondria were always presented as a reticular network (Fig. 5). The morphology of mitochondria was observed by adding 5 μM **AIE-MitoGreen-1** to the culture media from day 1 to 5, respectively. There was almost no change in the mitochondria morphology throughout the whole process. Taken together, these results have shown that **AIE-MitoGreen-1** is a highly suitable imaging agent for directly visualizing the mitochondria morphology and localization, and it is able to identify the differentiation stages of brown adipose cells. The photostability of **AIE-MitoGreen-1** was also tested through continuous scanning by confocal microscope, and the signal loss of **AIE-MitoGreen-1** is less than 10% in ~ 5 min under constant laser exposure (Fig. S3). As the pH in mitochondria is in the range of 7–8, the physical stability of **AIE-MitoGreen-1** was tested in buffer solutions with pH of 7 and 8, and no obvious changes in their UV absorption were observed after 24 hours, indicating the good stability of the probe (Fig. S4).

In summary, we report a novel fluorescent probe **AIE-MitoGreen-1** with AIE characteristics for specific mitochondrial imaging. It is easy to synthesize, and has significant advantages in cell permeability, low background signal, good cellular retention and low toxicity, enabling the real-time continuous monitoring of mitochondria morphology without washing steps. This probe has been used for identifying the differentiation stages of brown adipose cells in a quick and easy manner, showing that the mitochondria undergo significant changes from a reticular, tubular organization to a punctate morphology during the process. Fine tuning of the targeting ligands will yield more specific probes for monitoring various biological processes.

Acknowledgments

We thank the Singapore National Research Foundation (R-279-000-390-281), the SMART (R279-000-378-592), Institute of Materials Research and Engineering (IMRE/12-8P1103), intramural funding from Singapore Institute for Clinical Sciences (A*STAR), the Research Grants Council of Hong Kong (HKUST2/CRF/10 and N_HKUST620/11) and Guangdong Innovative Research Team Program (201101C0105067115) for financial support. We are also grateful to Drs. Yu-Hua Tseng and Kai Ge for the brown preadipose cell line WT-1.

References

1. (a) P. Lee, M. M. Swarbrick, and K. K. Ho, *Endocr Rev.*, 2013, **34**, 413-438; (b) A. Bartelt and J. Heeren, *Nat. Rev. Endocrinol.*, 2014, **10**, 24–36.
2. Y. I. Chen, A. M. Cypess, C. A. Sass, A. L. Brownell, K. T. Jokivarsi, C. R. Kahn and K. K. Kwong, *Obesity (Silver Spring)*, 2012, **20**, 1519–1526.
3. B. A. D. Neto, J. R. Correa and R. G. Silva, *RSC Adv.*, 2013, **3**, 5291–5301.
4. M. E. Lidell, M. J. Betz, O. D. Leinhard, M. Heglind, L. Elander, M. Slawik, T. Mussack, D. Nilsson, T. Romu, P. Nuutila, K. A. Virtanen, F. Beuschlein, A. Persson, M. Borga and S. Enerback, *Nat. Med.*, 2013, **19**, 631–634.
5. K. Okamoto, P. S. Perlman and R. A. Butow, *Methods Cell Biol.*, 2001, **65**, 277–283.
6. M. Liesa and O. S. Shirihai, *Cell Metab.*, 2013, **17**, 491–506.
7. (a) L. F. Yousif, K. M. Stewart and S. O. Kelley, *Chembiochem*, 2009, **10**, 1939–1950; (b) N. Jiang, J. Fan, T. Liu, J. Cao, B. Qiao, J. Wang, P. Gao and X. Peng, *Chem. Commun.*, 2013, **49**, 10620–10622.
8. (a) W. Tang, Y. Xiang and A. Tong, *J. Org. Chem.*, 2009, **74**, 2163–2166; (b) R. Wei, P. Song and A. Tong, *J. Phys. Chem. C*, 2013, **117**, 3467–3474.
9. N. Zhao, M. Li, Y. Yan, J. W. Y. Lam, Y. L. Zhang, Y. S. Zhao, K. S. Wong and B. Z. Tang, *J. Mater. Chem C*, 2013, **1**, 4640–4646.
10. (a) D. Ding, K. Li, B. Liu and B. Z. Tang, *Acc. Chem. Res.*, 2013, **46**, 2441-2453; (b) C. W. T. Leung, Y. Hong, S. Chen, E. Zhao, J. W. Lam and B. Z. Tang, *J. Am. Chem. Soc.*, 2013, **135**, 62–65; (c) Y. N. Hong, J. W. Y. Lam and B. Z. Tang, *Chem. Soc. Rev.*, 2011, **40**, 5361–5388.
11. (a) J. E. Kwon and S. Y. Park, *Adv. Mater.*, 2011, **23**, 3615–3642; (b) J. Wu, W. Liu, J. Ge, H. Zhang and P. Wang, *Chem. Soc. Rev.*, 2011, **40**, 3483–3495; (c) J. Zhao, S. Ji, Y. Chen, H. Guo and P. Yang, *Phys. Chem. Chem. Phys.*, 2012, **14**, 8803–8817.
12. J. Klein, M. Fasshauer, M. Ito, B. B. Lowell, M. Benito and C. R. Kahn, *J. Biol. Chem.*, 1999, **274**, 34795–34802.